

# The Best of the Two Worlds: Harmonizing Semantic and Hash IDs for Sequential Recommendation

Ziwei Liu  
City University of Hong Kong  
Hong Kong, China  
lziwei2-c@my.cityu.edu.hk

Yejing Wang  
City University of Hong Kong  
Hong Kong, China  
yejing.wang@my.cityu.edu.hk

Qidong Liu  
Xi'an Jiaotong University &  
City University of Hong Kong  
Xi'an, China  
liuqidong@xjtu.edu.cn

Zijian Zhang  
City University of Hong Kong  
Hong Kong, China  
zhangzijian@jlu.edu.cn

Wei Huang  
Independent Researcher  
Beijing, China  
hwdzyx@gmail.com

Chong Chen  
Tsinghua University  
Beijing, China  
cstchenc@163.com

Xiangyu Zhao✉  
City University of Hong Kong  
Hong Kong, China  
xianzhao@cityu.edu.hk

## Abstract

Conventional Sequential Recommender Systems (SRS) typically assign unique Hash IDs (HID) to construct item embeddings. These HID embeddings effectively learn collaborative information from historical user-item interactions, making them vulnerable to situations where most items are rarely consumed (the long-tail problem). Recent methods that incorporate auxiliary information often suffer from noisy collaborative sharing caused by co-occurrence signals or semantic homogeneity caused by flat dense embeddings. Semantic IDs (SIDs), with their capability of code sharing and multi-granular semantic modeling, provide a promising alternative. However, the collaborative overwhelming phenomenon hinders the further development of SID-based methods. The quantization mechanisms commonly compromise the uniqueness of identifiers required for modeling head items, creating a performance seesaw between head and tail items. To address this dilemma, we propose  $H^2Rec$ , a novel framework that harmonizes the SID and HID. Specifically, we devise a dual-branch modeling architecture that enables the model to capture both the multi-granular semantics within SID while preserving the unique collaborative identity of HID. Furthermore, we introduce a dual-level alignment strategy that bridges the two representations, facilitating knowledge transfer and supporting robust preference modeling. Extensive experiments on three real-world datasets show that  $H^2Rec$  effectively balances recommendation

✉Corresponding authors.

Permission to make digital or hard copies of all or part of this work for personal or classroom use is granted without fee provided that copies are not made or distributed for profit or commercial advantage and that copies bear this notice and the full citation on the first page. Copyrights for components of this work owned by others than ACM must be honored. Abstracting with credit is permitted. To copy otherwise, or republish, to post on servers or to redistribute to lists, requires prior specific permission and/or a fee. Request permissions from permissions@acm.org.  
Conference'17, Washington, DC, USA

© 2026 ACM.  
ACM ISBN 978-1-4503-8332-5/26/08  
<https://doi.org/xxx>

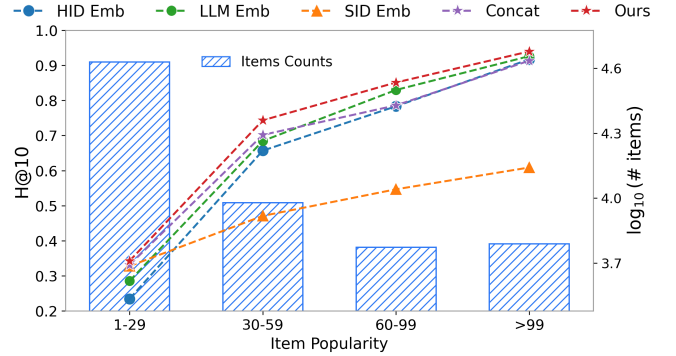


**Figure 1: Performance comparison with SASRec on Yelp (item popularity breakdown). The marker indicates the method type (●: HID-based, ▲: SID-based, ★: hybrid).**

quality for both head and tail items while surpassing the existing baselines. The implementation code can be found online<sup>1</sup>.

## Keywords

Sequential Recommendation; Information Retrieval

## ACM Reference Format:

Ziwei Liu, Yejing Wang, Qidong Liu, Zijian Zhang, Wei Huang, Chong Chen, and Xiangyu Zhao✉. 2026. The Best of the Two Worlds: Harmonizing Semantic and Hash IDs for Sequential Recommendation. In . ACM, New York, NY, USA, 11 pages. <https://doi.org/xxx>

## 1 Introduction

Sequential recommender systems (SRS) aim to predict users' next interactions based on their historical behaviors and are widely deployed across digital platforms such as e-commerce [2] and streaming media [5]. In conventional SRS frameworks, e.g., BERT4Rec [24], GRU4Rec [10], and SASRec [12], items are assigned unique identifiers (IDs) to enable hash-based lookup [29]. These hash IDs (HID)

<sup>1</sup><https://github.com/ziwliu8/H2Rec>

are then mapped to high-dimensional embeddings that encode collaborative information from historical interactions, allowing the model to learn users’ preferences effectively.

However, HID-based SRS suffer from a long-standing drawback: the long-tail item problem. As illustrated in Figure 1, HID embeddings (the blue line) degrade significantly for items with sparse interactions (tail items), which account for more than 70% of the whole item set. This observation confirms that traditional collaborative filtering methods [3] struggle to learn reliable representations for tail items due to insufficient data [29]. To address this issue, prior studies [9, 13] exploit co-occurrence patterns and enhance tail items by leveraging information from popular items interacted with by the same user. Although effective to some extent, these approaches overlook the semantic information embedded in item descriptions. Moreover, co-occurrence signals can be unreliable in real-world scenarios [20]. For example, accidental clicks produce misleading collaborative information, causing tail items to inherit noise from semantically unrelated popular items. This leads to the **① Noisy Collaborative Sharing** problem.

Recent advances in large language models (LLM) provide a promising avenue to mitigate this issue by enriching HID embeddings with semantic information [19, 36]. LLM-based item encoders extract both semantic features from items’ textual attributes and LLM’s general world knowledge [8, 17, 18], thereby deriving better item representation. We take the powerful LLM-ESR [18] as our baseline, denoted as “LLM Emb”. As shown in the green line of Figure 1, it achieves an improved performance across all item-popularity groups. However, LLM compresses all textual information into a single dense vector. We argue that this “flat” representation induces a single-granularity bottleneck. Here, we define the semantic granularity as the level of abstraction at which item semantics are expressed. A single dense embedding inevitably entangles coarse-grained semantics with fine-grained nuances, making it difficult to distinguish subtle differences among semantically similar items. This limitation gives rise to the **② Semantic Homogeneity** problem.

To simultaneously address these problems, recent work [31, 35] has turned to Semantic IDs (SID) for recommendation. Unlike HID, SID are generated by decomposing dense semantic embeddings (e.g., from LLMs) into discrete code sequences through vector quantization techniques such as RQ-VAE [14]. Crucially, the quantization hierarchy unfolds the dense embedding into multi-granular semantic views. Each residual level corresponds to a distinct abstraction of semantics, forming multiple implicit views rather than explicit metadata such as category or brand. This structure is theoretically appealing: shared codes at the same layer aggregate collaborative signals among semantically related items, mitigating **Noisy Collaborative Sharing**. Meanwhile, multi-granular codes offer finer semantic distinctions, alleviating the **Semantic Homogeneity** problem.

Despite these advantages, existing SID-based methods [6, 15, 16, 25, 32, 33] typically replace HID with SID or fuse them using simple concatenation or contrastive learning. Such strategies fail to fully exploit the potential of SID and are hindered by the **Collaborative Overwhelming** phenomenon. This phenomenon stems from the quantization process, which inevitably introduces code collisions

(e.g., multiple items share the same SID). These collisions compromise the uniqueness of ID-item mappings, confusing the model with inflated user-item connections. This effect is particularly pronounced for ‘head’ items with abundant interactions, as evidenced by the orange line in Figure 1. Consequently, Figure 1 reveals an intrinsic trade-off: pure SID lack the uniqueness required for head items, while pure HID lack the semantic information to benefit tail items. This underscores the need for a harmonized framework that integrates the strengths of both paradigms to achieve the best of two worlds.

In this paper, we propose a framework with **Harmonized Semantic and Hash IDs for Sequential Recommendation (H<sup>2</sup>Rec)**. Our framework employs a dual-branch architecture with dual-level alignment. Specifically, the SID branch includes a multi-granularity fusion network that constructs fine-grained semantic representations, addressing the **Semantic Homogeneity** problem. The HID branch incorporates a multi-granularity cross-attention network that selectively injects semantic signals into HID embeddings, preventing the **Collaborative Overwhelming** phenomenon. In addition, we introduce a Dual-level Alignment Strategy to harmonize the two spaces: a code-guided alignment loss at the item level to mitigate **Noisy Collaborative Sharing**, and a masked sequence granularity loss at the user level to enhance preference modeling. It is important to note that our framework is quantization-agnostic and model-agnostic, making it compatible with different quantization mechanisms and SRS architectures. Our contributions are summarized as follows:

- We identify the **Collaborative Overwhelming** phenomenon in SID-based methods, revealing a fundamental seesaw between the identifier uniqueness required for head items and the semantic needed for tail items.
- We propose **H<sup>2</sup>Rec**, a dual-branch framework that harmonizes HID and SID. By combining our multi-granularity modules with the Dual-level Alignment Strategy, H<sup>2</sup>Rec effectively addresses the limitations of each identifier type.
- Extensive experiments on three real-world datasets demonstrate that H<sup>2</sup>Rec significantly outperforms state-of-the-art baselines and achieves robust performance across head and tail items.

## 2 Preliminary

### 2.1 Problem Definition

The sequential recommendation aims to predict the next interacted items based on the historical record. Specifically, we can derive the interaction sequence for a specific user  $u \in \mathcal{U}$ , denoted as  $S_u = \{v_1, \dots, v_N\}$ , where  $v_i \in \mathcal{V}$  represents the interacted item  $i$  in the item set  $\mathcal{V}$ , and  $N$  represents the length of the interaction sequence. Correspondingly, we define the problem of SRS as:

$$\arg \max_{v_i \in \mathcal{V}} P(v_{N+1} = v_i | S_u) \quad (1)$$

### 2.2 Semantic IDs Generation

Vector Quantization has been widely used to generate the SID from the original embedding [7]. In our settings, we directly take the widely used Residual Quantized Variational Autoencoder (RQ-VAE) [14] as our SID generator, following the previous work [22].

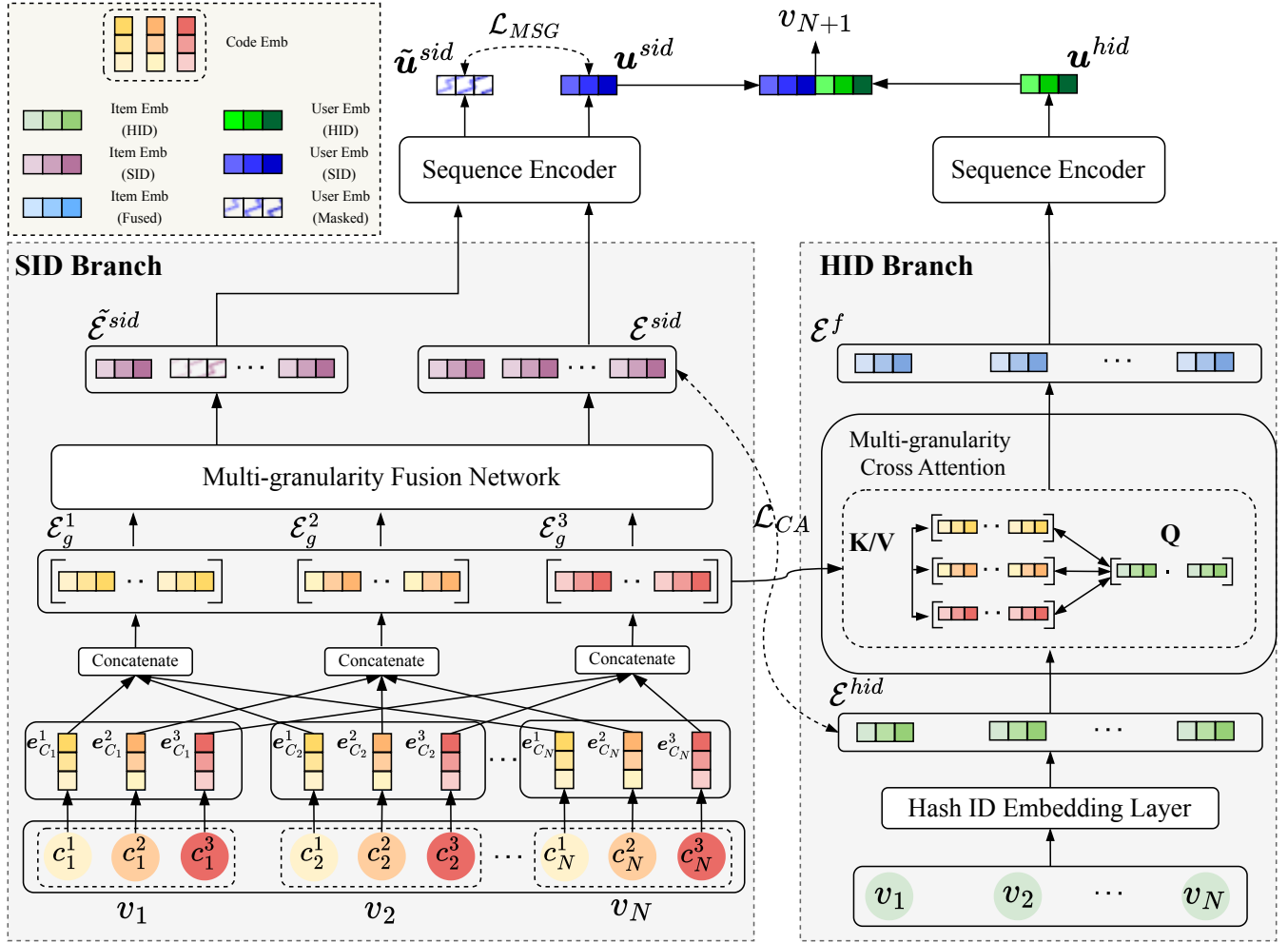


Figure 2: The framework overview for H<sup>2</sup>Rec. In this figure, we set  $L = 3$ .

Specifically, for a semantic embedding  $e_{LLM}$  derived from a language model encoder, we leverage RQ-VAE to quantize it into  $L$  semantic codes, where  $L$  denotes the number of code layers. Specifically, the item  $v_i$  can be represented as a tuple  $C_i = \{c_i^1, \dots, c_i^L\}$ , where  $c_i^l$  is a single code whose embedding  $e_{c_i^l}^l$  is the corresponding slice of codebook embedding  $E_C^l$ .

### 3 Methodology

In this section, we introduce the architecture of the proposed H<sup>2</sup>Rec. We begin with an overview of the framework, followed by detailed illustrations of its dual-branch structure and dual-level alignment. At last, the training and inference procedure is specified.

#### 3.1 Overview

The overview of our proposed framework is illustrated in Figure 2. To harmonize the two types of identifiers, we first devise a **Dual-branch Modeling** architecture. In the **SID Branch**, we employ an RQ-VAE framework, which maps textual attributes into  $L$  discrete code levels, to construct our Semantic code embeddings. Then, to

construct multi-granular representations, the generated code embeddings of the item sequence are concatenated based on their corresponding code levels, forming  $L$ -granularity sequences. With the proposed **Multi-granularity Fusion Network**, these sequences are then adaptively aggregated into a final fine-grained SID embedding sequence. Finally, a sequence encoder is employed to generate the user representation for SID branch, denoted as  $u^{sid}$ . In the **HID branch**, we first leverage a learnable embedding layer to derive the HID item embedding. After that, we introduce the **Multi-granularity Cross Attention Network**. Using the unique HID as the query, this module selectively incorporates essential semantic information from SID while preserving the uniqueness of head items, successfully generating an information-fused embedding sequence. Finally, another sequence encoder is applied on the fused embedding sequence to derive the user representation  $u^{hid}$  in the HID branch.

To further optimize the whole architecture, a **Dual-level Alignment Strategy** is proposed. At the item level, we design a **Code-Guided Alignment** loss that aligns the collaborative and semantic spaces with well-designed sample selection. This module allows

tail items to borrow high-quality collaborative signals from semantically similar head items without introducing noise. At the user level, to ensure robust user representation, we randomly mask a subset of granularities to obtain the masked user representation  $\tilde{\mathbf{u}}^{sid}$ . Then, we construct a **Masked Sequence Granularity Loss** to enhance internal correlations among multi-granular semantics.

At last, the mutually enhanced HID and SID user representations, i.e.,  $\mathbf{u}^{hid}$  and  $\mathbf{u}^{sid}$ , are fused to derive the recommendation scores.

## 3.2 Dual-branch Modeling

In this section, we present our dual-branch modeling, featuring the SID branch and the HID branch, to leverage the complementary benefits of the two different IDs.

**3.2.1 SID Branch.** To acquire the semantic code embeddings for each item, we first derive semantic embeddings from the item’s textual attributes by leveraging Large Language Models (LLM) [19]. Specifically, we convert item attributes into textual instructions and obtain the representations of all items, denoted as  $\mathbf{E}_{LLM} \in \mathbb{R}^{|V| \times d_{llm}}$ , using open-resource LLM [1, 27] or the public API, such as text-embedding-ada-002<sup>2</sup>. Subsequently, the RQ-VAE framework is trained to derive the semantic codes  $\mathbf{C}_i$  together with their corresponding codebook embedding matrices  $\mathbf{E}_C$  as mentioned in Section 2.2. The semantic code embeddings for item  $i$  are then retrieved from the  $l$  codebook embedding matrices through look-up operations, denoted as  $[\mathbf{e}_{C_1}^l, \dots, \mathbf{e}_{C_N}^l]$ . After that, we introduce the multi-granularity fusion network in our SID branch to generate more fine-grained SID representations. In this module, we first group the code embeddings of all items strictly by their code levels. The embedding sequence for each code level can be formulated as a separate granularity:  $\mathcal{E}_g^l = [\mathbf{e}_{C_1}^l, \mathbf{e}_{C_2}^l \dots, \mathbf{e}_{C_N}^l]$ , where  $l$  denotes a specific code level in semantic codes. Since the user intent is dynamically shifting, a fixed integration strategy is suboptimal. Therefore, we design an adaptive mechanism that leverages the user’s interaction context to assign importance weights to different code-level granularities. Formally, we use the embedding of the user’s last interacted item, denoted as  $\mathbf{e}_N^{hid} \in \mathbb{R}^d$ , from the HID embedding sequence to serve as the query anchor for the current intent. To ensure training stability and incorporate the prior knowledge that coarse-grained semantics are generally more robust, we introduce a learnable residual bias vector  $\mathbf{b}_{prior} \in \mathbb{R}^L$ , where  $L$  is the number of code levels. The unnormalized importance scores  $\mathbf{s} \in \mathbb{R}^L$  can then be computed via a Multi-Layer Perceptron (MLP) structure as follows:

$$\mathbf{s} = \mathbf{W}_2 (\sigma(\mathbf{W}_1 [\mathbf{e}_N; \mathbf{b}_{prior}] + \mathbf{b}_1)) + \mathbf{b}_2 + \mathbf{b}_{prior} \quad (2)$$

where “ $\cdot$ ” represents the concatenation operation,  $\mathbf{W}_1 \in \mathbb{R}^{d_h \times (d+L)}$ ,  $\mathbf{W}_2 \in \mathbb{R}^{L \times d_h}$ ,  $\mathbf{b}_1 \in \mathbb{R}^{d_h}$  and  $\mathbf{b}_2 \in \mathbb{R}^L$  are the weight matrices and biases. The residual addition of  $\mathbf{b}_{prior}$  explicitly enforces the model to respect the residual structure of SID generated by RQ-VAE, especially during the early training stages. Then, we normalize the scores into importance weights  $\alpha$  and derive the final SID item embedding sequence  $\mathcal{E}^{sid} = [\mathbf{e}_1^{sid}, \dots, \mathbf{e}_N^{sid}]$ :

$$\alpha_l = \frac{\exp(s_l)}{\sum_{k=1}^L \exp(s_k)}, \quad \mathcal{E}^{sid} = \sum_{l=1}^L \alpha_l \cdot \mathcal{E}_g^l \quad (3)$$

<sup>2</sup><https://platform.openai.com/docs/guides/embeddings>

Finally, we employ an independent sequence encoder, i.e.,  $f_{\theta^1}$  and acquire the final user representation  $\mathbf{u}^{sid}$  for our SID branch.

**3.2.2 HID Branch.** First, we derive the item embedding for the HID branch by employing a learnable item embedding layer and update it by absorbing the collaborative information from historical user-item interactions. Let  $\mathbf{E}_{hid} \in \mathbb{R}^{|V| \times d}$  represents the HID embedding layer of the item. Then, the item embedding sequence  $\mathcal{E}^{hid} = [\mathbf{e}_1^{hid}, \dots, \mathbf{e}_N^{hid}]$  can be derived by extracting the corresponding rows from  $\mathbf{E}_{hid}$ . To inject nuanced, multi-granular semantic information back into the HID item embedding, we propose the multi-granularity cross attention, which effectively mitigates the Collaborative Overwhelming phenomenon highlighted in Section 1. Formally, we treat the HID item embedding sequence  $\mathcal{E}^{hid}$  as the query anchor, while treating the multi-granular SID item embedding sequences  $\mathcal{E}_g^l$  as the key-value pairs. This strategy allows the model to utilize the unique HID as a query to selectively retrieve and inject semantic information from SID, thereby preventing the uniqueness of popular items from being overwhelmed by the shared semantic codes.

Specifically, for each code level  $l$ , we first project the collaborative and semantic sequences into distinct subspaces using learnable weight matrices  $\mathbf{W}^Q \in \mathbb{R}^{d \times d}$ ,  $\mathbf{W}^K \in \mathbb{R}^{d \times d}$ ,  $\mathbf{W}^V \in \mathbb{R}^{d \times d}$ , which can be formulated as:

$$\mathbf{Q} = \mathcal{E}^{hid} \mathbf{W}^Q, \quad \mathbf{K}_l = \mathcal{E}_g^l \mathbf{W}^K, \quad \mathbf{V}_l = \mathcal{E}_g^l \mathbf{W}^V \quad (4)$$

Based on these projections, we derive the final fused embedding sequence  $\mathcal{E}^f$  by aggregating the granularity-specific attention outputs, weighted by the user’s intent-aware scores  $\alpha_l$  derived in Equation (3). Crucially, a residual connection is employed to add back the original HID item embedding sequence:

$$\mathcal{E}^f = \sum_{l=1}^L \alpha_l \cdot \left( \text{softmax} \left( \frac{\mathbf{Q} \mathbf{K}_l^\top}{\sqrt{d}} \right) \mathbf{V}_l \right) + \mathcal{E}^{hid} \quad (5)$$

Through this unified aggregation, the framework leverages both the HID’s strength in maintaining uniqueness for popular items and the SID’s capability to enrich tail items via weighted granular semantics. Finally, a sequence encoder  $f_{\theta^2}$  is employed on the fused item embedding sequence to derive the comprehensive user representation  $\mathbf{u}^{hid}$  for the HID branch.

## 3.3 Dual-level Alignment

To further enhance the representation ability of each branch, we propose a dual-level alignment approach, featuring a code-guided alignment loss at the item level and a masked sequence granularity loss at the user level.

**3.3.1 Code-guided Alignment Loss.** To mitigate the Noisy Collaborative Sharing, we aim to align the semantic and collaborative spaces. A straightforward solution is to adopt a standard contrastive learning objective that pulls the SID item embedding  $\mathbf{e}_i^{sid}$  and HID item embedding  $\mathbf{e}_i^{hid}$  of the same item  $i$  closer while pushing them away from negative samples. This 1-to-1 alignment explicitly transfers the collaborative signals unique to item  $i$  into its semantic representation, formulated as:

$$\mathcal{L}_{align} = -\frac{1}{B} \sum_{i=1}^B \log \frac{\exp(\cos(\mathbf{e}_i^{sid}, \mathbf{e}_i^{hid})/\tau)}{\sum_{j=1}^B \mathbb{I}[i \neq j] \exp(\cos(\mathbf{e}_i^{sid}, \mathbf{e}_j^{hid})/\tau)} \quad (6)$$

where  $B$  denotes the batch size,  $\cos(\cdot, \cdot)$  represents the cosine similarity, and  $\tau$  is the temperature coefficient.

However, this strict 1-to-1 mapping is insufficient for our goal: enabling long-tail items (which lack interaction data) to implicitly “borrow” high-quality collaborative signals from semantically similar head items. To address this, we expand the objective from a 1-to-1 alignment to a 1-to-many code-guided alignment. This strategy leverages the multi-granular nature of SID to identify semantically similar items and inject their collaborative signals into the anchor item. Additionally, to capture sequential dependencies, we also incorporate items appearing within the local context window as positive samples. Specifically, we construct a unified positive set  $\mathcal{P}(i)$  for item  $i$  by incorporating two additional sources: (1)  $\mathcal{P}_C(i)$ , the set of items sharing  $p$  levels of semantic codes with item  $i$ ; and (2)  $\mathcal{P}_H(i)$ , the set of items appearing within the co-occurrence context window  $o$ . Let  $\mathcal{P}(i) = \{i\} \cup \mathcal{P}_C(i) \cup \mathcal{P}_H(i)$ . We then reconstruct the objective to maximize the cumulative similarity between the anchor SID item embedding and all positive HID item embeddings:

$$\mathcal{L}_{CA}^1 = -\frac{1}{B} \sum_{i=1}^B \log \frac{\sum_{k \in \mathcal{P}(i)} \exp(\cos(\mathbf{e}_i^{sid}, \mathbf{e}_k^{hid})/\tau)}{\sum_{j=1}^B \exp(\cos(\mathbf{e}_i^{sid}, \mathbf{e}_j^{hid})/\tau)} \quad (7)$$

Intuitively, this mechanism enables information sharing exclusively among items that exhibit verified semantic similarity (via shared codes) or collaborative proximity (via co-occurrence). To obtain the second part of the alignment loss, we simply exchange the roles of  $\mathbf{e}^{sid}$  and  $\mathbf{e}^{hid}$ , yielding  $\mathcal{L}_{CA}^2$ . The final alignment loss is then expressed as:  $\mathcal{L}_{CA} = \mathcal{L}_{CA}^1 + \mathcal{L}_{CA}^2$ .

**3.3.2 Masked Sequence Granularity Loss.** Specifically, for each user interaction sequence, we construct two different views: a global view and a granularity-masked view. The global view preserves the complete multi-granular semantic codes. In contrast, in the granularity-masked view, we randomly sample a target granularity index  $m \in [1, L]$ , where  $L$  denotes the total number of code levels, and replace the embedding sequence at this level with a learnable mask token, resulting in the masked sequence  $\tilde{\mathcal{E}}^{sid}$ . Both views are then processed through the multi-granularity fusion network and subsequently fed into the shared sequence encoder  $f_{\theta^1}(\cdot)$  to derive the global representation  $\mathbf{u}^{sid}$  and the masked representation  $\tilde{\mathbf{u}}^{sid}$ . To ensure that the model can implicitly infer the missing semantic information from the remaining context and other granularities, we maximize the mutual information between the two resulting representations. Formally, for a batch of  $N$  users, we minimize the distance between the positive pair  $(\mathbf{u}_i^{sid}, \tilde{\mathbf{u}}_i^{sid})$  while pushing apart negative pairs involving representations from other users:

$$\mathcal{L}_{MSG}^1 = -\frac{1}{N} \sum_{i=1}^N \log \frac{\exp(\cos(\mathbf{u}_i^{sid}, \tilde{\mathbf{u}}_i^{sid})/\tau)}{\sum_{j=1}^N \exp(\cos(\mathbf{u}_i^{sid}, \tilde{\mathbf{u}}_j^{sid})/\tau)} \quad (8)$$

where  $\cos(\cdot, \cdot)$  denotes the cosine similarity, and  $\tau$  is the temperature coefficient. For the other side of our proposed objective, we exchange the position of the masked user representation  $\tilde{\mathbf{u}}^{sid}$  and original user representation  $\mathbf{u}^{sid}$  to derive the  $\mathcal{L}_{MSG}^2$ . Thereby, the final loss can be formulated as:  $\mathcal{L}_{MSG} = \mathcal{L}_{MSG}^1 + \mathcal{L}_{MSG}^2$ .

---

#### Algorithm 1 Train and Inference Procedures of H<sup>2</sup>Rec.

---

**Require:** User set  $\mathcal{U}$ , Item set  $\mathcal{I}$

- 1: Indicate the backbone SRS  $f_{\theta^1}$  and  $f_{\theta^2}$ .
- 2: Indicate the weights of  $\mathcal{L}_{CA}$  and  $\mathcal{L}_{MSG}$ .
- 3: Derive semantic embedding  $E_{LLM}$  by LLM and codebook embedding matrix  $E_C$  by RQ-VAE.

##### Training

- 4: Initialize the HID item embeddings by dimension-reduced  $E_{LLM}$ .
  - 5: Initialize the semantic code embeddings by looking up through the  $E_C$ .
  - 6: **for** a batch of users  $\mathcal{U}_B$  in  $\mathcal{U}$  **do**
  - 7:   Get the embedding sequence of different granularities from code embeddings.
  - 8:   Generate the weight  $\alpha_l$  for different granularities by Equation (2).
  - 9:   Derive the final SID item embedding sequence  $\mathcal{E}^{hid}$  by Equation (3).
  - 10:   Get the fused embedding sequence  $\mathcal{E}^f$  by Equation (5).
  - 11:   Get the user representation in SID branch and HID branch, i.e.,  $\mathbf{u}^{sid}$  and  $\mathbf{u}^{hid}$ .
  - 12:   Calculate the probability score of ground-truth and negative items by Equation (9).
  - 13:   Calculate the ranking loss by Equation (10).
  - 14:   Calculate the  $\mathcal{L}_{CA}$  by Equation (7) and  $\mathcal{L}_{MSG}$  by Equation (8).
  - 15:   Sum the  $\mathcal{L}_{rec}$ ,  $\mathcal{L}_{CA}$ , and  $\mathcal{L}_{MSG}$ . Then, update the parameters.
  - 16: **end for**
  - Inference**
  - 17: Load  $E_{LLM}$ ,  $E_C$ , and  $\alpha_l$  for item embedding layers and other parameters.
  - 18: **for** a batch of users  $\mathcal{U}_B$  in  $\mathcal{U}$  **do**
  - 19:   Get the user representation in SID branch and HID branch, i.e.,  $\mathbf{u}^{sid}$  and  $\mathbf{u}^{hid}$ .
  - 20:   Calculate the probability score by Equation (9) and give the final next-item prediction.
  - 21: **end for**
- 

### 3.4 Training and Inference

**3.4.1 Training.** As described in Section 3.2.2 and Section 3.2.1, we first obtain the embedding sequences  $\mathcal{E}^{hid}$  and  $\mathcal{E}^{sid}$  for each branch and leverage two individual sequence encoder to derive the final  $\mathbf{u}^{sid}$  and  $\mathbf{u}^{hid}$ . After that, we can compute the probability of recommending item  $j$  to user  $u$  based on the fused representations as:

$$P(v_{N+1} = v_j | \mathcal{S}_u) = [\mathbf{e}_j^{sid} : \mathbf{e}_j^{hid}]^\top [\mathbf{u}^{sid} : \mathbf{u}^{hid}] \quad (9)$$

where  $:$  denotes the concatenation operator. Based on these scores, we optimize the model using a pairwise ranking loss:

$$\mathcal{L}_{rec} = - \sum_{u \in \mathcal{U}} \sum_{j=1}^N \log \sigma(P(v_{j+1} = v^+ | \mathcal{S}_u) - P(v_{j+1} = v^- | \mathcal{S}_u)) \quad (10)$$

where  $v^+$  and  $v^-$  respectively represent the ground-truth item and the corresponding negative item.

**Table 1: The statistics of datasets**

Dataset	# Users	# Items	Sparsity	Avg.length
Yelp	15,720	11,383	99.89%	12.23
Beauty	52,204	57,289	99.92%	7.56
Instrument	40,644	30,676	99.97%	8.01

Finally, the overall training objective combines the main recommendation loss with the code-guided alignment Loss and the masked sequence granularity loss:

$$\mathcal{L} = \mathcal{L}_{rec} + \beta \cdot \mathcal{L}_{CA} + \gamma \cdot \mathcal{L}_{MSG} \quad (11)$$

where  $\beta$  and  $\gamma$  are hyperparameters controlling the contributions of the two auxiliary objectives.

**4.4.2 Inference.** During inference, since the SID and the associated codebook embeddings are cached in advance, we directly compute recommendation scores using Equation (9). For completeness, we summarize the full training and inference pipeline in Algorithm 1.

## 4 Experiment

### 4.1 Experiment Settings

**4.1.1 Datasets.** We apply three real-world datasets to evaluate the effectiveness of our proposed H<sup>2</sup>Rec, *i.e.*, Yelp, Amazon Beauty, and Amazon Instrument. For data preprocessing and splitting, we follow the previous SRS works [18, 21]. The statistics are presented in Table 1.

**4.1.2 Baselines.** To validate the superiority of H<sup>2</sup>Rec, we conduct our comparison experiment with various up-to-date baselines under three categories.

- HID Embedding: BERT4Rec [24], SASRec [12], MELT [13], and LLM-ESR [18].
- SID Embedding: PG-SID [37], SPM-SID [23], CCFRec [16] and PSRQ+MCCA [30], which is denoted as PSRQ for simplicity.
- Hybrid Embedding: URL4DR [15], MME-SID [32], and PCR-CA [25].

**4.1.3 Implementation Details.** We implement all our experiments on a single RTX 4090 24G GPU, while the basic software requirements are Python 3.11 and PyTorch 2.4-2204.  $\beta$  and  $\gamma$  are all searched from {0.1, 0.3, 0.5, 0.7, 0.9}. Please find more details of our implementation code at the repository <sup>3</sup>.

**4.1.4 Evaluation Metrics.** To provide a comprehensive view of our framework, following existing research [18, 20, 34], we split the items into tail and head groups by selecting the top 20% items as head items and regarding the rest as tail items. For detailed evaluation for each group, we adopt the commonly used *Hit Rate* and *Normalized Discounted Cumulative Gain*, all truncated at 10, denoted as  $H@10$  and  $N@10$  respectively. To ensure the robustness of the experimental results, all the presented results are the average of the three runs with random seeds {42, 43, 44}.

<sup>3</sup><https://github.com/ziwliu8/H2Rec>

### 4.2 Overall Performance

In this section, we evaluate the performance of our model across different item popularity groups on three public datasets. As shown in Table 2, H<sup>2</sup>Rec achieves substantial improvements over state-of-the-art baselines, with relative gains ranging from 1.29% to 11.88% across multiple evaluation metrics. We provide a more detailed analysis below.

**4.2.1 Overall.** From Table 2, following H<sup>2</sup>Rec, the Hybrid Embedding methods (*e.g.*, PCR-CA and MME-SID) and the LLM-based method (*i.e.*, LLM-ESR) generally yield the next-best performance. This observation suggests that although infusing LLM-derived knowledge into HID or simply combining multiple embeddings improves performance, such strategies remain insufficient without explicit and fine-grained alignment between the two spaces.

For SID Embedding baselines, we observe a clear performance disparity. Although the recently proposed SFM-SID and PG-SID adopt more sophisticated mechanisms to enhance semantic representations, they generally underperform compared to CCFRec and PSRQ. This indicates that strengthening semantic quality alone is inadequate without a recommendation-oriented architectural design. Among SID-based methods, CCFRec performs notably comparable to the HID-based SASRec. Its advantage is attributed to progressively incorporating semantic embeddings from multiple attribute dimensions, yielding finer item distinctions than the sub-vector grouping strategies in SFM-SID and PG-SID. Nevertheless, despite these improvements, single-view methods (first seven columns) are consistently inferior to hybrid approaches (last four columns), further demonstrating the necessity of integrating both SID and HID in a unified framework.

**4.2.2 Popularity Breakdown.** HID Embedding-based methods (*e.g.*, SASRec and LLM-ESR) excel on Head items due to abundant interaction data, yet suffer drastic performance declines on the Tail group, revealing their reliance on dense collaborative signals. Conversely, SID-based methods (*e.g.*, PSRQ and CCFRec) effectively address sparsity for Tail items by leveraging semantic information for collaborative sharing. For example, PSRQ and CCFRec significantly surpass SASRec on Tail items. However, their performance on the Head group remains limited, primarily due to the inherently coarse-grained nature of SID and the quantization-induced ID collisions.

In contrast, H<sup>2</sup>Rec eliminates this trade-off. It achieves the best results in the Tail group, substantially outperforming the SID-based baselines, while simultaneously maintaining state-of-the-art performance on the Head group compared to the HID-based methods. This demonstrates that H<sup>2</sup>Rec successfully transfers semantic knowledge to cold items without compromising the model’s capability to capture fine-grained collaborative information for popular items, illustrating the effectiveness of our proposed modules.

### 4.3 Ablation Study

To assess the contribution of each proposed component, we conduct an ablation study by selectively removing individual modules while keeping the remaining architecture unchanged. The variants are defined as follows: (1) *w/o Fusion Network*: Removes the proposed multi-granularity fusion network and replaces it with fixed weights

**Table 2: Overall performance of the proposed H<sup>2</sup>Rec. The best results are bold, and the second-best are underlined. “\*\*” indicates the improvements are statistically significant (i.e., two-sided t-test with  $p < 0.05$ ) over baselines.**

Dataset	Group	Metric	HID Emb				SID Emb				Hybrid Emb			Ours	Improv.
			BERT4Rec	SASRec	MELT	LLM-ESR	SFM-SID	PG-SID	CCFRec	PSRQ	URL4DR	MME-SID	PCR-CA	H <sup>2</sup> Rec	%
Yelp	Overall	H@10	0.5314	0.5940	0.6101	<u>0.6573</u>	0.4727	0.4881	0.5947	0.5438	0.6402	0.6431	0.6447	<b>0.6692*</b>	1.81%
		N@10	0.3147	0.3601	0.3394	<u>0.4102</u>	0.3148	0.3251	0.3694	0.3422	0.3776	0.3884	0.3971	<b>0.4272*</b>	4.14%
	Tail	H@10	0.0177	0.1175	0.1223	0.1802	0.2441	0.2492	0.2478	<u>0.2543</u>	0.1957	0.2215	0.2032	<b>0.2693*</b>	5.90%
		N@10	0.0068	0.0588	0.0599	0.0676	0.1162	0.1186	0.1171	<u>0.1210</u>	0.0914	0.1103	0.0954	<b>0.1306*</b>	7.93%
	Head	H@10	0.6919	0.7413	0.7790	<u>0.8059</u>	0.5218	0.5334	0.7071	0.6398	0.7699	0.7702	0.7748	<b>0.8324*</b>	3.29%
		N@10	0.3876	0.4592	0.4745	<u>0.5122</u>	0.3079	0.3147	0.4243	0.3721	0.4735	0.4823	0.4860	<b>0.5483*</b>	7.05%
Beauty	Overall	H@10	0.3992	0.4401	0.4890	<u>0.5544</u>	0.3715	0.3836	0.4398	0.4038	0.5464	0.5509	0.5539	<b>0.5742*</b>	3.57%
		N@10	0.2401	0.3043	0.3357	<u>0.3702</u>	0.2617	0.2703	0.3021	0.2845	0.3675	0.3617	0.3673	<b>0.3957*</b>	6.89%
	Tail	H@10	0.0123	0.0921	0.1536	0.2198	0.2208	0.2254	0.2238	<u>0.2300</u>	0.1967	0.2177	0.2048	<b>0.2557*</b>	11.17%
		N@10	0.0052	0.0675	0.0877	0.1074	0.1355	0.1383	0.1323	<u>0.1411</u>	0.1105	0.1404	0.1342	<b>0.1524*</b>	8.01%
	Head	H@10	0.4988	0.5291	0.5815	0.6377	0.4388	0.4485	0.5099	0.4875	0.6299	0.6393	<u>0.6419</u>	<b>0.6502*</b>	1.29%
		N@10	0.2971	0.4007	0.4106	0.4289	0.3251	0.3323	0.3887	0.3612	0.4300	0.4379	<u>0.4401</u>	<b>0.4538*</b>	3.11%
Instrument	Overall	H@10	0.4601	0.5057	0.5510	0.5881	0.4312	0.4453	0.5078	0.4687	0.6005	0.6044	<u>0.6072</u>	<b>0.6184*</b>	1.84%
		N@10	0.3213	0.3442	0.3622	0.3809	0.2908	0.3003	0.3376	0.3161	0.4024	0.4027	<u>0.4056</u>	<b>0.4153*</b>	2.39%
	Tail	H@10	0.0199	0.0489	0.0766	0.0998	0.2058	0.2101	0.2099	<u>0.2144</u>	0.1605	0.2044	0.1827	<b>0.2382*</b>	11.10%
		N@10	0.0143	0.0257	0.0459	0.0549	0.0990	0.1010	0.0907	<u>0.1031</u>	0.0828	0.0991	0.1025	<b>0.1233*</b>	11.88%
	Head	H@10	0.5028	0.5806	0.6188	0.6676	0.5569	0.5693	0.5629	0.6188	0.6643	0.6646	<u>0.6701</u>	<b>0.6832*</b>	1.95%
		N@10	0.3190	0.3764	0.4237	0.4522	0.3813	0.3898	0.4192	0.4237	0.4483	0.4498	<u>0.4543</u>	<b>0.4638*</b>	2.09%

**Table 3: Performance comparison on the Yelp Dataset. “FN” denotes the fusion network, and “MCA” is the multi-granularity cross attention. Best results are in bold.**

Variants	Overall		Tail		Head	
	N@10	H@10	N@10	H@10	N@10	H@10
<b>H<sup>2</sup>Rec</b>	<b>0.4272</b>	<b>0.6692</b>	<b>0.1306</b>	<b>0.2693</b>	<b>0.5483</b>	<b>0.8324</b>
w/o FN	0.4123	0.6605	0.1013	0.2347	0.5404	0.8208
w/o $\mathcal{L}_{CA}$	0.4044	0.6455	0.1067	0.2161	0.4920	0.7719
w/o MCA	0.4072	0.6523	0.1105	0.2190	0.5218	0.8077
w/o $\mathcal{L}_{MSG}$	0.4202	0.6667	0.1091	0.2285	0.5398	0.8258

across different granularities. (2) w/o  $\mathcal{L}_{CA}$ : Eliminates the code-guided alignment loss. (3) w/o *Multi-granularity Cross Attention*: Removes the multi-granularity cross-attention module to examine the importance of information transfer between the HID and SID branches. (4) w/o  $\mathcal{L}_{MSG}$ : Removes the masked sequence granularity loss to evaluate its contribution. We evaluate these variants on the Yelp dataset, and the results are reported in Table 3. Based on the empirical observations, we summarize the findings below:

- **Effectiveness of Fusion and MSG Loss.** Both the fusion network and  $\mathcal{L}_{MSG}$  improve the semantic representation quality. The improved SID embeddings lead to better performance on Tail items, demonstrating the importance of learning adaptive and robust multi-granular semantics.
- **Role of Cross-branch Interaction.** Removing the MCA module results in a notable performance degradation on Head items. This confirms that cross-branch information transfer is essential, as it enables the HID branch to selectively absorb beneficial multi-granular semantic information without losing identifier uniqueness.
- **Importance of Code-guided Alignment.** The removal of  $\mathcal{L}_{CA}$  causes declines across both Head and Tail groups, indicating that

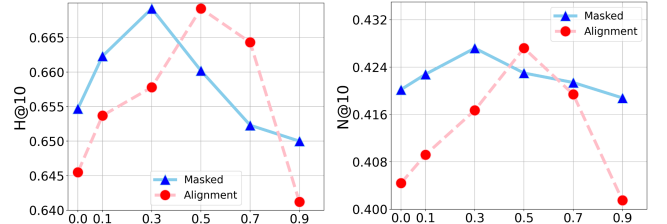


**Figure 3: Hyper-parameter Results on Yelp Dataset. Note that “Masked” represents the  $\mathcal{L}_{MSG}$  while “Alignment” represents the  $\mathcal{L}_{CA}$ .**

our alignment strategy effectively facilitates accurate and noise-resistant collaborative information sharing among semantically related items.

These results demonstrate that the proposed H<sup>2</sup>Rec framework successfully leverages the complementary strengths of HID and SID, thereby addressing the aforementioned problems outlined in Section 1.

#### 4.4 Hyperparameter Analysis

We analyze the sensitivity of two key hyperparameters: the weight of the alignment loss  $\beta$  and the weight of the granularity-masked loss  $\gamma$ . The results on the Yelp dataset are presented in Figure 4. Both hyperparameters exhibit clear and consistent trends:

**4.4.1 Alignment Weight  $\beta$ .** Performance increases as  $\beta$  grows and reaches the optimum around  $\beta = 0.5$ . A small value of  $\beta$  compromises the code-guided alignment, resulting in an insufficient transfer of collaborative signals to semantically similar Tail items. Conversely, an excessively large  $\beta$  causes the semantic space to over-align to the collaborative space, introducing noise and harming generalization.



**Table 4: Impact of the semantic code-matching threshold  $p$  on the Yelp dataset. Best results are highlighted in bold.**

code num	Overall		Tail		Head	
	N@10	H@10	N@10	H@10	N@10	H@10
Removed	0.4095	0.6505	0.1177	0.2211	0.4970	0.7769
1	0.4059	0.6473	0.1058	0.2044	0.4955	0.7712
2	0.4199	0.6582	0.1204	0.2591	0.5385	0.8247
3 (Ours)	<b>0.4272</b>	<b>0.6692</b>	<b>0.1306</b>	<b>0.2693</b>	<b>0.5483</b>	<b>0.8324</b>

**Table 5: Impact of the context window size  $o$  on the Yelp dataset. Best results are highlighted in bold.**

context	Overall		Tail		Head	
	N@10	H@10	N@10	H@10	N@10	H@10
Removed	0.4148	0.6522	0.1176	0.2230	0.5072	0.7911
1	0.4190	0.6523	0.1208	0.2294	0.5205	0.8062
3 (Ours)	<b>0.4272</b>	<b>0.6692</b>	<b>0.1306</b>	<b>0.2693</b>	<b>0.5483</b>	<b>0.8324</b>
5	0.4205	0.6637	0.1244	0.2638	0.5441	0.8299

**4.4.2 Granularity Weight  $\gamma$ .** The performance for our masked sequence granularity loss peaks at  $\gamma = 0.3$ . As an auxiliary regularizer designed to enforce internal consistency,  $\mathcal{L}_{MSG}$  requires a balanced weight: values that are too low fail to ensure representation robustness, while excessive weights interfere with the primary recommendation task.

#### 4.5 In-depth Analysis for $\mathcal{L}_{CA}$

To further validate the effectiveness of our code-guided strategy in mitigating the noisy collaborative sharing problem, we analyze the influence of two key design factors in  $\mathcal{L}_{CA}$ : the code-matching threshold  $p$  and the context window size  $o$ .

**4.5.1 Impact of Code Matching Threshold.** Table 4 shows that using  $p = 1$ , which considers only the coarsest semantic layer, leads to notable performance degradation. This observation indicates that overly coarse categories tend to group many weakly related items together, thereby introducing noise into the positive set. Increasing the threshold to  $p = 3$  yields significant improvements across all metrics, especially for Tail items. This demonstrates that deeper semantic matching is crucial for filtering out noise and ensuring that only truly similar items share collaborative signals.

**4.5.2 Impact of Context Window Size.** As shown in Table 5, expanding the co-occurrence window improves performance up to  $o = 3$ , confirming the utility of incorporating local, sequentially related items as additional positives. However, when the window is enlarged to  $o = 5$ , the model begins to include less relevant items, which results in a performance drop.

These results verify that our design, which combines multi-level semantic matching with local collaborative context, is essential for accurate and noise-robust alignment within  $\mathcal{L}_{CA}$ .

#### 4.6 Group Analysis

For a more fine-grained analysis, we further divide the original head–tail item group in Table 2 into five groups according to item

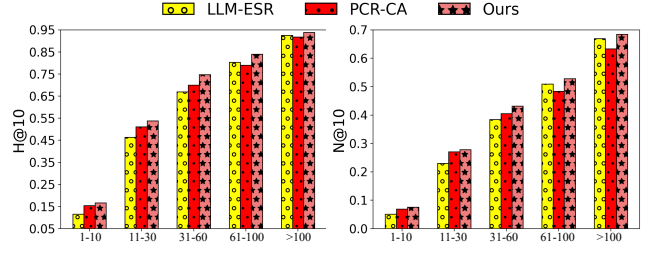


**Figure 4: Detailed results in different item groups on the Yelp dataset.**

**Table 6: Performance comparison of  $H^2$ Rec with different quantization mechanisms on the Yelp Dataset. Best results are highlighted in bold.**

Model	Overall		Tail		Head	
	N@10	H@10	N@10	H@10	N@10	H@10
VQ +	0.4091	0.6531	0.0943	0.1986	0.5018	0.7869
PQ +	0.4124	0.6597	0.1091	0.2285	0.5118	0.7958
RQ +	<b>0.4272</b>	<b>0.6692</b>	<b>0.1306</b>	<b>0.2693</b>	<b>0.5483</b>	<b>0.8324</b>

popularity. The results are illustrated in Figure ?? . From the figure, we observe that no matter for  $H@10$  or  $N@10$ , PCR-CA, which adopts a hybrid embedding mechanism, achieves a clear performance gain over the LLM-enhanced method (*i.e.*, LLM-ESR) in groups with popularity lower than 60 (the first three grouped columns). In addition, its performance in groups with popularity greater than 60 (the last two grouped columns) is almost on par with that of LLM-ESR, demonstrating the advantage of hybrid embedding approaches.

In contrast, our method further leverages a dual-branch architecture together with a dual-level alignment strategy to achieve additional optimization. As a result, it consistently outperforms all existing methods across all popularity groups.

#### 4.7 Generality Validation

**4.7.1 Quantization Mechanism Analysis.** In this section, we compare the performance of  $H^2$ Rec using SID generated by three commonly adopted quantization mechanisms: VQ [4], PQ [11], and RQ [14]. As shown in Table 6,  $H^2$ Rec maintains competitive performance under all configurations, demonstrating the robustness and general applicability of our design. We further provide insights into the performance differences:

- **RQ achieves the strongest performance** because its residual coding structure naturally captures residual semantic granularity. This fine-grained representation helps mitigate data sparsity, leading to performance gains on Tail items.
- **PQ provides moderate improvements** since it partitions the embedding space into subspaces, offering a balanced trade-off between semantic precision and code compactness.
- **VQ performs the weakest** because mapping each item to a single discrete code causes severe semantic collapse, reducing item uniqueness across both head and tail groups.



**Table 7: Performance comparison on the Yelp dataset with different backbones. The best results are highlighted in bold.**

Backbone	Model	Overall		Tail Items		Popular Items	
		N@10	H@10	N@10	H@10	N@10	H@10
GRU4Rec	PCR-CA	0.3613	0.5988	0.0745	0.1889	0.4311	0.7204
	LLM-ESR	0.3627	0.6075	0.0482	0.0952	0.4491	0.7338
	<b>Ours</b>	<b>0.3804</b>	<b>0.6239</b>	<b>0.0983</b>	<b>0.2058</b>	<b>0.4634</b>	<b>0.7470</b>
BERT4Rec	PCR-CA	0.4173	0.6604	0.0720	0.1689	0.5346	0.8175
	LLM-ESR	0.4205	0.6635	0.0503	0.1247	0.5444	0.8223
	<b>Ours</b>	<b>0.4298</b>	<b>0.6724</b>	<b>0.0991</b>	<b>0.1735</b>	<b>0.5545</b>	<b>0.8344</b>

**Table 8: Performance comparison of different SID settings on the Yelp Dataset. "Coll." represents the collision rate of SID, while "Util." represents the utilization rate.**

Settings	Overall		Tail		Head		Coll.%	Util.%
	N@10	H@10	N@10	H@10	N@10	H@10		
3x128	0.4145	0.6510	0.1152	0.2480	0.5365	0.8150	33.92	0.54
3x256	0.4192	0.6585	0.1215	0.2565	0.5402	0.8215	29.92	0.068
3x512	0.4235	0.6640	0.1268	0.2630	0.5445	0.8270	25.85	0.008
4x128	0.4272	0.6692	0.1306	0.2693	0.5483	0.8324	22.28	0.004
4x256	<b>0.4338</b>	<b>0.6785</b>	<b>0.1385</b>	<b>0.2790</b>	<b>0.5540</b>	<b>0.8410</b>	11.87	<0.001

Despite these differences, all variants achieve consistently strong results, even under the least expressive VQ setting. This demonstrates that H<sup>2</sup>Rec can effectively exploit semantic signals regardless of the underlying quantization mechanism, confirming the generalizability and plug-and-play nature of our framework.

**4.7.2 Backbone Analysis.** To further verify the model-agnostic nature of our framework, we evaluate H<sup>2</sup>Rec under two widely adopted sequential recommendation backbones, *i.e.*, GRU4Rec and BERT4Rec. We also compare it with two competitive hybrid baselines, PCR-CA and LLM-ESR, under the same backbone for fair comparison. The results shown in Table 7 demonstrate that, across both RNN-based and Transformer-based architectures, H<sup>2</sup>Rec consistently surpasses all baselines. This confirms that our framework is not restricted to a specific encoder design and can function as a universal, plug-and-play enhancement module for various SRS.

## 4.8 Semantic Code Analysis

In this section, we present how our proposed H<sup>2</sup>Rec performs under SID with different qualities. We conduct our experiments on two aspects, *i.e.*, code layers and codebook size. Since there are too many combinations to choose from, we only test the SID with representative settings. The results are reported in Table 8. From Table 8, we observe that expanding codebook capacity yields consistent improvements, which stems from the significant reduction in collision rates. Lower collision rates mitigate the semantic ambiguity, thereby enhancing the distinctiveness of item representations. However, this performance gain comes at the cost of codebook redundancy. As observed, the  $4 \times 256$  setting suffers from an extremely low utilization rate compared to smaller settings. Therefore, to strike a balance between minimizing collision rates (to ensure distinctiveness) and maintaining a reasonable utilization rate (to ensure efficiency), we set  $4 \times 128$  as the default setting for all the experiments above.

## 5 Related Work

### 5.1 Sequential Recommender Systems

The primary goal of Sequential Recommender Systems (SRS) is to model dynamic user preferences based on historical interaction sequences for next-item prediction [2, 5]. Early methodologies adapted neural architectures to this task, including RNN-based GRU4Rec [10] and CNN-based Caser [26]. Following the breakthrough of Transformers in natural language processing, self-attention mechanisms [28], exemplified by SASRec [12] and BERT4Rec [24], have become the dominant paradigm due to their superior ability to capture long-range dependencies. Despite their success, conventional ID-based frameworks face intrinsic limitations. First, for tail items with sparse interactions, the model often struggles to learn reliable representations [29]. While prior studies attempt to leverage co-occurrence patterns to enhance tail items [9, 13], these signals can be unreliable in real-world scenarios, leading to the **Noisy Collaborative Sharing** problem where tail items inherit misleading signals from unrelated popular items [20].

To mitigate data sparsity, recent research has incorporated Large Language Models (LLM) to encode textual attributes into item representations [17–19]. However, most existing approaches compress detailed textual descriptions into a single dense vector. As argued in Section 1, this “flat” representation suffers from a single-granularity bottleneck, entangling coarse-grained semantics with fine-grained nuances. Consequently, the model fails to distinguish subtle discrepancies between semantically similar items, leading to the **Semantic Homogeneity** problem. Our proposed H<sup>2</sup>Rec addresses these issues by introducing harmonized Semantic and Hash IDs, leveraging a dual-level alignment strategy to refine both representation spaces.

### 5.2 Semantic IDs Enhanced Sequential Recommendation

To overcome the limitations of Hash IDs (HID) and dense embeddings, researchers have investigated the paradigm of Semantic IDs (SID). SID are typically generated by decomposing dense semantic features (*e.g.*, from LLMs) into discrete code sequences via vector quantization techniques like RQ-VAE [14]. Theoretically, this discretization process naturally unfolds the flat embedding into multi-granular semantic views, offering a structural advantage for recommendation. Methods such as VQRec [6], SPM-SID [23], and PG-SID [37] leverage the code-sharing nature of SID, where semantically similar items share common code indices. By aggregating signals based on semantic content rather than unreliable co-occurrence, these methods aim to mitigate **Noisy Collaborative Sharing**. Furthermore, approaches such as CCFRec [16] and PSRQ [30] utilize the hierarchical structure of SID to capture explicit semantic units, aiming to alleviate the **Semantic Homogeneity** problem.

However, the effective utilization of SID remains a challenge. Current state-of-the-art methods typically adopt a substitution strategy [6, 33] or fuse identifiers via simple concatenation or contrastive learning [15, 25, 32]. These straightforward integration strategies overlook a critical trade-off: the **Collaborative Overwhelming Phenomenon**. The quantization process inevitably

introduces code collisions and lossy compression, which compromises the uniqueness of item identifiers. In pure or lightly fused SID frameworks, shared semantic codes tend to "overwhelm" the unique distinctiveness required for popular (head) items, resulting in performance degradation where ID uniqueness is crucial. In contrast, H<sup>2</sup>Rec employs a dual-branch framework that harmonizes semantic and hash IDs. By synergizing multi-granularity cross-attention with a Dual-level Alignment strategy, our approach effectively balances the uniqueness of HID with the semantic generalization of SID.

## 6 Conclusion

In this work, we investigated the fundamental trade-off between identifier uniqueness and semantic generalization in sequential recommendation, and formally identified the **Collaborative Overwhelming** phenomenon. To address the resulting performance imbalance between head and tail items, we proposed **H<sup>2</sup>Rec**, a dual-branch framework that harmonizes Hash IDs (HID) and Semantic IDs (SID). By integrating a multi-granularity fusion network with a multi-granularity cross attention Network, H<sup>2</sup>Rec effectively captures fine-grained semantic distinctions while preserving the collaborative specificity necessary for popular items, alleviating the **Semantic Homogeneous** problem. Moreover, our dual-level alignment strategy bridges the semantic and collaborative spaces, enabling long-tail items to borrow high-quality signals and mitigating the **Noisy Collaborative Sharing** problem. Extensive experiments on three real-world datasets demonstrate that H<sup>2</sup>Rec consistently outperforms state-of-the-art baselines. Importantly, it breaks the performance bottleneck by achieving substantial gains on tail items without sacrificing performance on head items.

## References

- [1] Jinze Bai, Shuai Bai, Yunfei Chu, Zeyu Cui, Kai Dang, Xiaodong Deng, Yang Fan, Wenbin Ge, Yu Han, Fei Huang, et al. 2023. Qwen technical report. *arXiv preprint arXiv:2309.16609* (2023).
- [2] Qiwei Chen, Huan Zhao, Wei Li, Pipei Huang, and Wenwu Ou. 2019. Behavior sequence transformer for e-commerce recommendation in alibaba. In *Proceedings of the 1st international workshop on deep learning practice for high-dimensional sparse data*. 1–4.
- [3] Hui Fang, Danning Zhang, Yiheng Shu, and Guibing Guo. 2020. Deep learning for sequential recommendation: Algorithms, influential factors, and evaluations. *ACM Transactions on Information Systems (TOIS)* 39, 1 (2020), 1–42.
- [4] Robert Gray. 1984. Vector quantization. *IEEE Assp Magazine* 1, 2 (1984), 4–29.
- [5] Lei Guo, Hongzhi Yin, Qinyong Wang, Tong Chen, Alexander Zhou, and Nguyen Quoc Viet Hung. 2019. Streaming session-based recommendation. In *Proceedings of the 25th ACM SIGKDD international conference on knowledge discovery & data mining*. 1569–1577.
- [6] Yupeng Hou, Zhankui He, Julian McAuley, and Wayne Xin Zhao. 2023. Learning vector-quantized item representation for transferable sequential recommenders. In *Proceedings of the ACM Web Conference 2023*. 1162–1171.
- [7] Yupeng Hou, An Zhang, Leheng Sheng, Zhengyi Yang, Xiang Wang, Tat-Seng Chua, and Julian McAuley. 2025. Generative Recommendation Models: Progress and Directions. In *Companion Proceedings of the ACM on Web Conference 2025*. 13–16.
- [8] Jun Hu, Wenwen Xia, Xiaolu Zhang, Chilin Fu, Weichang Wu, Zhaoxin Huan, Ang Li, Zuoli Tang, and Jun Zhou. 2024. Enhancing sequential recommendation via llm-based semantic embedding learning. In *Companion Proceedings of the ACM Web Conference 2024*. 103–111.
- [9] Seongwon Jang, Hoyeop Lee, Hyunsook Cho, and Sehee Chung. 2020. Cities: Contextual inference of tail-item embeddings for sequential recommendation. In *2020 IEEE International Conference on Data Mining (ICDM)*. IEEE, 202–211.
- [10] Dietmar Jannach and Malte Ludewig. 2017. When recurrent neural networks meet the neighborhood for session-based recommendation. In *Proceedings of the eleventh ACM conference on recommender systems*. 306–310.
- [11] Herve Jegou, Matthijs Douze, and Cordelia Schmid. 2010. Product quantization for nearest neighbor search. *IEEE transactions on pattern analysis and machine intelligence* 33, 1 (2010), 117–128.
- [12] Wang-Cheng Kang and Julian McAuley. 2018. Self-attentive sequential recommendation. In *2018 IEEE international conference on data mining (ICDM)*. IEEE, 197–206.
- [13] Kibum Kim, Dongmin Hyun, Sukwon Yun, and Chanyoung Park. 2023. Melt: Mutual enhancement of long-tailed user and item for sequential recommendation. In *Proceedings of the 46th international ACM SIGIR conference on Research and development in information retrieval*. 68–77.
- [14] Doyup Lee, Chiheon Kim, Saehoon Kim, Minsu Cho, and Wook-Shin Han. 2022. Autoregressive image generation using residual quantization. In *Proceedings of the IEEE/CVF conference on computer vision and pattern recognition*. 11523–11532.
- [15] Guanyu Lin, Zhigang Hua, Tao Feng, Shuang Yang, Bo Long, and Jiaxuan You. 2025. Unified semantic and ID representation learning for deep recommenders. *arXiv preprint arXiv:2502.16474* (2025).
- [16] Enze Liu, Bowen Zheng, Wayne Xin Zhao, and Ji-Rong Wen. 2025. Bridging Textual-Collaborative Gap through Semantic Codes for Sequential Recommendation. In *Proceedings of the 31st ACM SIGKDD Conference on Knowledge Discovery and Data Mining V. 2*. 1788–1798.
- [17] Qidong Liu, Xian Wu, Wanyu Wang, Yejing Wang, Yuanshao Zhu, Xiangyu Zhao, Feng Tian, and Yefeng Zheng. 2025. Llmemb: Large language model can be a good embedding generator for sequential recommendation. In *Proceedings of the AAAI Conference on Artificial Intelligence*. Vol. 39. 12183–12191.
- [18] Qidong Liu, Xian Wu, Yejing Wang, Zijian Zhang, Feng Tian, Yefeng Zheng, and Xiangyu Zhao. 2024. Llm-esr: Large language models enhancement for long-tailed sequential recommendation. *Advances in Neural Information Processing Systems* 37 (2024), 26701–26727.
- [19] Qidong Liu, Xiangyu Zhao, Yuhao Wang, Yejing Wang, Zijian Zhang, Yuqi Sun, Xiang Li, Maolin Wang, Pengyue Jia, Chong Chen, et al. 2024. Large Language Model Enhanced Recommender Systems: A Survey. *arXiv preprint arXiv:2412.13432* (2024).
- [20] Siyi Liu and Yujia Zheng. 2020. Long-tail session-based recommendation. In *Proceedings of the 14th ACM conference on recommender systems*. 509–514.
- [21] Ziwei Liu, Qidong Liu, Yejing Wang, Wanyu Wang, Pengyue Jia, Maolin Wang, Zitao Liu, Yi Chang, and Xiangyu Zhao. 2025. SIGMA: Selective Gated Mamba for Sequential Recommendation. *Proceedings of the AAAI Conference on Artificial Intelligence* 39, 12 (Apr. 2025), 12264–12272. <https://doi.org/10.1609/aaai.v39i12.33336>
- [22] Shashank Rajput, Nikhil Mehta, Anima Singh, Raghunandan Hulikal Keshavan, Trung Vu, Lukasz Heldt, Lichan Hong, Yi Tay, Vinh Tran, Jonah Samost, et al. 2023. Recommender systems with generative retrieval. *Advances in Neural Information Processing Systems* 36 (2023), 10299–10315.
- [23] Anima Singh, Trung Vu, Nikhil Mehta, Raghunandan Keshavan, Maheswaran Sathiamoorthy, Yilin Zheng, Lichan Hong, Lukasz Heldt, Li Wei, Devansh Tandon, et al. 2024. Better generalization with semantic ids: A case study in ranking for recommendations. In *Proceedings of the 18th ACM Conference on Recommender Systems*. 1039–1044.
- [24] Fei Sun, Jun Liu, Jian Wu, Changhua Pei, Xiao Lin, Wenwu Ou, and Peng Jiang. 2019. BERT4Rec: Sequential recommendation with bidirectional encoder representations from transformer. In *Proceedings of the 28th ACM international conference on information and knowledge management*. 1441–1450.
- [25] Bin Tan, Wangyao Ge, Yidi Wang, Xin Liu, Jeff Burtoft, Hao Fan, and Hui Wang. 2025. PCR-CA: Parallel Codebook Representations with Contrastive Alignment for Multiple-Category App Recommendation. *arXiv preprint arXiv:2508.18166* (2025).
- [26] Jiaxi Tang and Ke Wang. 2018. Personalized top-n sequential recommendation via convolutional sequence embedding. In *Proceedings of the eleventh ACM international conference on web search and data mining*. 565–573.
- [27] Hugo Touvron, Thibaut Lavril, Gautier Izacard, Xavier Martinet, Marie-Anne Lachaux, Timothée Lacroix, Baptiste Rozière, Naman Goyal, Eric Hambro, Faisal Azhar, et al. 2023. Llama: Open and efficient foundation language models. *arXiv preprint arXiv:2302.13971* (2023).
- [28] Ashish Vaswani, Noam Shazeer, Niki Parmar, Jakob Uszkoreit, Llion Jones, Aidan N Gomez, Lukasz Kaiser, and Illia Polosukhin. 2017. Attention is all you need. *Advances in neural information processing systems* 30 (2017).
- [29] Shoujin Wang, Liang Hu, Yan Wang, Longbing Cao, Quan Z Sheng, and Mehmet Orgun. 2019. Sequential recommender systems: challenges, progress and prospects. *arXiv preprint arXiv:2001.04830* (2019).
- [30] Shijia Wang, Tianpei Ouyang, Qiang Xiao, Dongjing Wang, Yintao Ren, Songpei Xu, Da Guo, and Chuanjiang Luo. 2025. Progressive Semantic Residual Quantization for Multimodal-Joint Interest Modeling in Music Recommendation. *arXiv preprint arXiv:2508.20359* (2025).
- [31] Wenjie Wang, Xinyu Lin, Fuli Feng, Xiangnan He, and Tat-Seng Chua. 2023. Generative recommendation: Towards next-generation recommender paradigm. *arXiv preprint arXiv:2304.03516* (2023).
- [32] Yuhao Wang, Junwei Pan, Xinhang Li, Maolin Wang, Yuan Wang, Yue Liu, Dapeng Liu, Jie Jiang, and Xiangyu Zhao. 2025. Empowering Large Language Model for Sequential Recommendation via Multimodal Embeddings and Semantic IDs. *arXiv preprint arXiv:2509.02017* (2025).

- [33] Yi Xu, Moyu Zhang, Chaofan Fan, Jinxin Hu, Xiaochen Li, Yu Zhang, Xiaoyi Zeng, and Jing Zhang. 2025. MMQ-v2: Align, Denoise, and Amplify: Adaptive Behavior Mining for Semantic IDs Learning in Recommendation. *arXiv preprint arXiv:2510.25622* (2025).
- [34] Hongzhi Yin, Bin Cui, Jing Li, Junjie Yao, and Chen Chen. 2012. Challenging the long tail recommendation. *arXiv preprint arXiv:1205.6700* (2012).
- [35] An Zhang, Yuxin Chen, Leheng Sheng, Xiang Wang, and Tat-Seng Chua. 2024. On generative agents in recommendation. In *Proceedings of the 47th international ACM SIGIR conference on research and development in Information Retrieval*. 1807–1817.
- [36] Wayne Xin Zhao, Kun Zhou, Junyi Li, Tianyi Tang, Xiaolei Wang, Yupeng Hou, Yingqian Min, Beichen Zhang, Junjie Zhang, Zican Dong, et al. 2023. A survey of large language models. *arXiv preprint arXiv:2303.18223* 1, 2 (2023).
- [37] Carolina Zheng, Minhui Huang, Dmitrii Pedchenko, Kaushik Rangadurai, Siyu Wang, Fan Xia, Gaby Nahum, Jie Lei, Yang Yang, Tao Liu, et al. 2025. Enhancing embedding representation stability in recommendation systems with semantic id. In *Proceedings of the Nineteenth ACM Conference on Recommender Systems*. 954–957.